PREDICTION OF *IN VIVO* BONE FORMING POTENCY OF BONE MARROW-DERIVED HUMAN MESENCHYMAL STEM CELLS

Patricia Janicki, Stephane Boeuf, Eric Steck, Marcus Egermann, Philip Kasten§ and Wiltrud Richter*

Research Centre for Experimental Orthopaedics, Orthopaedic University Hospital Heidelberg, Heidelberg, Germany
§Current address: Department of Orthopaedic Surgery, University of Dresden, Dresden, Germany

Abstract

Human mesenchymal stem cells (MSC) have attracted much attention for tissue regeneration including repair of non-healing bone defects. Heterogeneity of MSC cultures and considerable donor variability however, still preclude standardised production of MSC and point on functional deficits for some human MSC populations. We aimed to identify functional correlates of donor-dependency of bone formation in order to develop a potency assay predicting the therapeutic capacity of human MSC before clinical transplantation. MSC from 29 donors were characterised *in vitro* and results were correlated to bone formation potency in a beta-tricalcium-phosphate (β-TCP)-scaffold after subcutaneous implantation into immunocompromised mice.

In contrast to osteogenic *in vitro* differentiation parameters, a doubling time below 43.23 hours allowed to predict ectopic bone formation at high sensitivity (81.8%) and specificity (100%). Enriched conditions adapted from embryonic stem cell expansion rescued bone formation of inferior MSC populations while growth arrest of potent MSC by mitomycin C abolished bone formation, establishing a causal relationship between neo-bone formation and growth. Gene expression profiling confirmed a key role for proliferation status for the bone forming ability suggesting that a rate limiting anabolism and open chromatin determined and predicted the therapeutic potency of culture-expanded MSC. Proliferation-based potency testing and switch to enriched expansion conditions may pave the way for standardised production of MSC for bone repair.

Key words: Bone tissue engineering, beta-tricalcium-phosphate, heterotopic bone formation, mesenchymal stem cell, cell proliferation, prediction, microarray.

*Address for correspondence:
Wiltrud Richter
Research Centre for Experimental Orthopaedics
Department of Orthopaedics
Trauma Surgery and Paraplegia
Orthopaedic University Hospital Heidelberg
Schlierbacher Landstrasse 200a,
D-69118 Heidelberg, Germany
Telephone Number: +49-(0)-6221-969253
FAX Number: +49-(0)-6221-969288
E-mail: Wiltrud.Richter@med.uni-heidelberg.de

Introduction

Mesenchymal stem cells (MSC) support the homeostasis of mesenchymal tissues and their trophic and mesengenic activities bear a high therapeutic potential for tissue regeneration. Reflecting the complexity of the stromal system in bone marrow, MSC populations expanded from marrow aspirates are heterogeneous in nature with the exact composition depending on the donor (Rickard *et al*., 1996; Majors *et al*., 1997; Muschler *et al.*, 2001), the individual aspirate (Lazarus *et al*., 1997; Muschler *et al*., 1997; Phinney *et al*., 1999; Muschler *et al*., 2001; Hernigou *et al*., 2006), applied isolation methods and expansion conditions, the latter of which differ largely among investigators (Phinney, 2002; Shahdadfar *et al*., 2005; Sotiropoulou *et al*., 2006; Mannello and Tonti, 2007; Wagner and Ho, 2007). Cloned populations of MSC demonstrate that only part of the cells is multipotent while the remaining population shows varied phenotypes (Russell *et al*., 2010). Increasing interest in the clinical use of MSC, however, demands standardised methods to produce cell populations of high regeneration capacity and accurate control of their therapeutic potential (Phinney, 2007; Caplan, 2009; Tarte *et al*., 2010). This includes the necessity to determine the therapeutic potency of every MSC population by an adequate assay before it may be transplanted.

MSC-based tissue engineering approaches have attracted attention in the context of bone repair since they were successfully used to bridge large bone defects in animal models (Bruder *et al*., 1998a; Bruder *et al*., 1998b). Bone formation by bone marrow-derived human MSC is, however, less robust compared to other species according to classical tests of heterotopic bone formation (Krebsbach *et al*., 1997), which further document a donor variability for human MSC populations (Mendes *et al*., 2002; Mendes *et al*., 2004; Siddappa *et al*., 2007; Siddappa *et al*., 2008; Matsushima *et al*., 2009). Parameters such as age, gender, medication or disease of the donor and the location of bone marrow harvest (Muschler *et al*., 2001; Stenderup *et al*., 2003; McLain *et al*., 2005; Siddappa *et al*., 2007) were considered as reasons for this undesired character of human MSC, pointing out functional deficits for human MSC populations from some donors compared to others. On the other hand, expansion conditions are likely to influence the overall cell composition (Martin *et al*., 1997; Muraglia *et al*., 1998; Kuznetsov *et al*., 2000) and the fitness of cells at the time of transplantation may strongly influence their actual bone forming potency *in vivo*. It is conceivable that patients treated with suboptimal MSC populations may develop poorer regeneration results or that cell-based treatment may even fail in spite of high

costs inflicted with this therapy. So far no tests are available to predict the potency of individual bone marrow-derived MSC populations to form bone *in vivo* in order to pave the way for standardised clinical use of MSC in bone repair. In addition, no rate-limiting cellular or molecular correlates of *in vivo* bone formation have been identified for human MSC.

While many studies addressed donor variations regarding growth and osteogenic *in vitro* potential of human MSC (Jaiswal *et al.*, 1997; Digirolamo *et al.*, 1999; Phinney *et al.*, 1999; Mendes *et al.*, 2004; Siddappa *et al.*, 2007), and predictors of successful *in vitro* osteogenesis of MSC have recently been reported (Platt *et al.*, 2009; Pietila *et al.*, 2010), no irrefutable positive correlation between *in vitro* parameters or molecular signatures of bone marrow-derived human MSC populations and *in vivo* bone formation have been identified.

This study was undertaken to unravel rate-limiting cellular and molecular aspects underlying the ectopic bone formation ability of human MSC. This test requires the use of a scaffold and a recently characterised beta-tricalcium-phosphate (β-TCP) was chosen, since it demonstrated superior potency compared with a hydroxyapatite/tricalcium-phosphate (HA/TCP) ceramic (Janicki *et al.*, 2010). In order to extract predictors applicable as clinically relevant potency assays, our approach was to expand human MSC from a large cohort of donors under standardised conditions. Donor characteristics, growth properties, *in vitro* differentiation potential and gene expression profile of each MSC population were determined and correlated to the *in vivo* bone formation. We identify a rate-limiting doubling time and molecular signature of open chromatin as highly predictive for *in vivo* bone formation, and establish a causal relationship between bone formation and growth allowing the rescue of inferior MSC populations for therapeutic use.

Materials and Methods

Cell isolation and cultivation

Human bone marrow cells were aspirated from the iliac crest or femur of 29 donors. Informed consent was obtained from all individuals and the study was approved by the local ethics committee. MSC were isolated from fresh bone marrow samples as described previously (Dickhut *et al.*, 2009). In short, density gradient isolated mononuclear cells were seeded in expansion medium (High-glucose Dulbecco's modified Eagle's medium (DMEM, Invitrogen, Karlsruhe, Germany), 2 % foetal calf serum (FCS, Biochrom, Germany), 40 % MCDB201, 0.02 µM dexamethasone, 0.1 mM ascorbic acid 2-phosphate, 2 % insulin-transferrin-sodium selenite media supplement (all Sigma-Aldrich, Steinheim, Germany), 100 U/mL penicillin and 100 µg/mL streptomycin (Biochrom, Berlin, Germany), 10 ng/mL recombinant human epidermal growth factor and recombinant human platelet-derived growth factor BB (both Strathmann Biotech, Hamburg, Germany) (Reyes *et al.*, 2001) at a density of 5 x10^5 cells/cm^2. Where indicated, mononucleated cells (n = 5

donors) were simultaneously seeded at a density of 1.25 x10^5 cells per cm^2 into 0.1 % gelatin-coated flasks in an embryonic stem cell (ES) medium (DMEM, 12.5 % FCS, 2 mM L-glutamine, 1 % non essential amino acids, 0.1 % 2-mercaptoethanol (Invitrogen), 100 U/mL penicillin, 100 µg/mL streptomycin, 4 ng/mL human fibroblast growth factor-2 (Active Bioscience, Hamburg, Germany)). 33 % of the ES medium was conditioned for 48 h by primary mouse embryo fibroblasts (PMEF-NL, Millipore, Molsheim, France). Standard culturing conditions were used (37 °C, 6 % CO$_2$) and the medium was changed twice a week. For culturing MSC were replated at a density of 4-6 x10^3 cells/cm^2.

Cell surface marker expression profiles and the multipotency were standardly determined for MSC populations, as described previously (Winter *et al.*, 2003; Dickhut *et al.*, 2009). Depending on the experimental setting, cells from passage 1, 2, 3 or 5 were used. For inhibition of cell proliferation at passage 2 (n = 4 donors) cells were treated for 2 h with medium containing 20 µg/mL mitomycin C (Sigma-Aldrich) and washed twice with PBS. Untreated and mitomycin C-treated MSC were then incubated with 1 % trypsin/ethylenediaminetetraacetic acid (Biochrom) solution, harvested, centrifuged, resuspended in PBS and used for experiments like WST-1 assay (replated in culture medium), osteogenesis *in vitro* (replated in induction medium) or ectopic transplantation (seeded on β-TCP granules).

Heterotopic *in vivo* bone formation assay

To allow broad characterisation of MSC from the first 20 donors in multiple assays at the time of transplantation, about 3 x10^7 cells were required from each donor. This number was usually reached at passage 3 (P3) allowing all assays to be started including β-TCP/MSC transplantation to assess heterotopic bone formation after 8 weeks.

Phase-pure (>95 %) β-TCP (Ca$_3$(PO$_4$)$_2$) granules (0.5-0.7 mm, RMS Foundation, Bettlach, Switzerland) with a porosity of 60 %, macropores of 100-500 µm and not specified micropores were sterilised for 6 h at 120 °C, and 10 mg granules were mixed with 1 x10^6 MSC and fibrin glue as described previously (Janicki *et al.*, 2010). Seeding efficiency was 98-99 % according to counting of MSC remaining after a first washing step of the constructs. Freshly prepared three-dimensional constructs consisting of β-TCP and MSC (2-4 per donor, n = 29 donors) were transplanted for 8 weeks into paravertebral subcutaneous pouches of 6-8 week old male severe combined immunodeficiency (SCID) mice (n = 45) (Charles River, Sulzfeld, Germany). According to the number of MSC populations cultured simultaneously, β-TCP/MSC constructs of one or two donors were transplanted into one animal. Two to four subcutaneous pouches were prepared per mouse and one construct per pouch was implanted. All procedures were performed according to the European Laboratory Animal Science guidelines. The experimental protocol was approved by the local animal experimentation committee (35-9185.81G-95/06). All animals survived the experimental period of 8 weeks.

Histological evaluation

β-TCP/MSC explants were fixed in Bouin´s solution for 2 days providing fixation and partial decalcification in one step (Kuznetsov *et al.*, 2000). Further, explants were dehydrated using graded alcohol series and embedded in paraffin. Sections were stained with haematoxylin and eosin (H&E, Chroma, Münster, Germany). Human cells were identified by detection of human-specific genomic Alu repeats using a digoxygenin-labelled probe, as previously described (Steck *et al.*, 2010). Briefly, paraffin sections were deparaffinised, rehydrated in alcohol and digested in 50 ng/mL proteinase K (Fermentas, St. Leon-Rot, Germany). After washing with PBS, sections were treated with 0.1 M triethanolamine hydrochloride pH 8 (Sigma-Aldrich) in 0.25 % acetic acid and pre-hybridised in hybridisation buffer containing 4x saline-sodium citrate (SSC), 1x Denhardt's solution, 5 % dextrane sulphate, 50 % deionised formamide, 100 µg/mL salmon sperm DNA and aqua bidest. Hybridisation buffer was replaced by fresh hybridisation buffer containing 0.2 ng/µL dioxigenin-labelled probe, sections were denaturated and immediately cooled. Hybridisation was carried out for 16 h in a wet chamber. Sections were washed twice in 2x SSC and twice in 0.1x SSC. Positive signals were detected by using anti-digoxygenin alkaline phosphatase-conjugated Fab fragments and nitro-blue-tetrazolium/5-Bromo-4-chloro-3-indolyl-phosphate (Roche, Mannheim, Germany) as substrate. Sections were counterstained with fast red (Chroma).

Osteogenic *in vitro* differentiation of human MSC

Per donor (n = 29 donors) 3.5×10^4 MSC per well were seeded in quadruplicates into 24-well plates and were incubated with high-glucose DMEM supplemented with 10 % FCS, 0.1 µM dexamethasone, 0.17 mM ascorbic acid 2-phosphate, 10 mM β-glycerophosphate (Sigma-Aldrich) and 1 % penicillin/streptomycin. At four time points (day 1, 7, 14, 21) two wells each were used for assessment of alkaline phosphatase (ALP) enzyme activity while two wells served to quantify mineralisation using alizarin red S staining.

Alkaline phosphatase activity assay

Cells were lysed with 1 % triton X-100 detergent (Sigma-Aldrich) in PBS, scraped off the plate and stored at -80 °C (two wells per donor and time point). ALP activity was assessed in duplicates by diluting two 50 µL samples with 50 µL ALP buffer (0.1 M glycine, 1 mM $MgCl_2$, 1 mM $ZnCl_2$, pH 10.4) each before incubation with 100 µL ALP buffer plus 1 mg/mL p-nitrophenylphosphate (p-NPP). The conversion to p-nitrophenol (p-NP) was measured spectrophotometrically at 405/490 nm after 1 h of incubation. Total protein concentration was determined by the Micro BCA™ Protein Assay Reagent Kit (Pierce Biotechnology, Rockford, IL, USA) according to manufacturer's instructions. The amount of p-NP divided by the amount of total protein normalised the specific amount of ALP.

Alizarin red S staining for calcification

Cells were fixed with 70 % ethanol and stained with 0.5 % alizarin red S (Chroma) (two wells per donor and time point). Monolayers were treated with 10 % hexadecetylpyridinium-chloride-monohydrate (CPC) and the eluted solution of each well was measured spectrophotometrically in duplicates at 570 nm. The amount of CPC was divided by the amount of total protein to normalise for cell quantity.

Evaluation of generation time

Generation time was calculated for each MSC donor population (n = 29) using the following formula: $G = (\log 2 \times T) / (\log Y - \log X)$. G stands for generation time [hours], T for time in culture per passage [hours], Y for cell number at harvesting time point, X for cell number at seeding time point.

^{3}H-thymidine proliferation assay

To analyse the proliferation rate, 4×10^3 MSC were seeded into 96-wells in triplicates in expansion medium (n = 29 donors). After 24 h, medium was replaced by fresh medium containing 0.25 µCi of [methyl-^{3}H]-thymidine (GE Healthcare, München, Germany) per well. After additional 18 h cells were washed, lysed with 1 % triton X-100 and transferred into tubes containing 2 mL scintillation cocktail (Perkin Elmer, Waltham, MA, USA). Radioactivity was measured by a WinSpectral 1414 Liquid Scintillation Counter (Perkin Elmer).

WST-1 assay

To analyse the vitality, 4×10^3 MSC were seeded into 96-wells in triplicates in expansion medium (n = 2 donors). Medium was replaced 24 h after seeding by 90 µL fresh medium and supplemented with 10 µL of 4-[3-(4-Iodophenyl)-2-(4-nitrophenyl)-2H-5-tetrazolio]-1,3-benzene disulfonate (WST-1, Roche, Mannheim, Germany) per well. MSC were incubated for 1 h at 37 °C according to manufacturer's instructions and the cleavage of WST-1 to formazan was measured spectrophotometrically at 450 nm.

Microarray analysis

Total RNA was isolated out of $0.6\text{-}3 \times 10^6$ expanded MSC (n = 8 populations with and n = 8 populations without the ability to form ectopic bone) at the time point of transplantation using RNeasy Mini kit according to manufacturer´s instructions (Qiagen, Hilden, Germany). The microarray analysis (Illumina Human Sentrix, Human Ref_8 v3.0) was performed at the Genomic & Proteomics Core Facility of the German Cancer Research Centre in Heidelberg, Germany. Briefly, cDNA was synthesised from 0.5 µg of total RNA, followed by an amplification/labelling step to synthesise a biotin-labelled cRNA. After purification and quality control, 0.75 µL of the labelled probes were hybridised to the BeadChips consisting of 24.495 transcripts and transcript variants. Data analysis was done by normalisation of the signals using the

quantile normalisation algorithm without background subtraction, and differentially regulated genes were defined by calculating the standard deviation differences of a given probe in a one-by-one comparison of both groups. Cluster analysis was adopted to find differences between MSC with and without bone forming capability. Log transformed signal intensities were calculated and submitted to average linkage hierarchical clustering using the Cluster and Treeview software (Eisen *et al.*, 1998). Significantly different expressed genes were annotated using open source Database for Annotation, Visualisation and Integrated Discovery (DAVID v6.7 (Dennis *et al.*, 2003; Huang *et al.*, 2009)).

Quantitative real-time polymerase chain reaction
First-strand cDNA was synthesised from 2 µg of total RNA using Omniscript reverse transcriptase (0.2 U/µL) and oligo(dT) primers (1 µM) (Qiagen) according to the manufacturer's instructions. The cDNA was quantified with a LightCycler 3 using LightCycler FastStart DNA Master SYBR Green I Kit (both Roche Diagnostics) according to the manufacturer's instructions. The following primers were used: β-actin: 5′-CTCTTCCAGCCTTCCTTCCT-3′, 5′-CGATCCACACGGAGTACTTG-3′; CDC20: 5′-CATTCGCATCTGGAATGTGT-3′, 5′-GCCTGAGATGAGCTCCTTGTA-3′; HIST2H2AA3: 5′-TACATGGCTGCGGTCCTC-3′, 5′-GGAGGTGACGAGGGATGAT-3′. The β-actin signal was used for normalisation.

Statistical analysis
Differences in outcome parameters were assessed by non-parametric two-tailed Mann-Whitney U test and a $p \leq 0.05$ was considered significant. For correlations between two categorial variables, the non-parametric Spearman´s rank correlation (r_s) was applied. To reflect the degree of linear relationship between two variables, the Pearson´s correlation (r_p) was adopted. To determine thresholds for ALP values and generation time in regard to bone formation, the receiver-operating characteristic (ROC) analysis was performed calculating sensitivity/specificity pairs by varying the decision threshold levels over the entire range of results (Metz *et al.*, 1973; Zweig and Campbell, 1993). Data analysis was performed with SPSS for Windows 16.0 (SPSS Inc., Chicago, IL, USA).

Results

Donor variability of heterotopic bone formation
While explants derived from the same donor showed little variation in neo-bone formation, a huge variability was evident for constructs from different donors. Overall, MSC from 11 out of 20 donors had formed bone (Table 1) with no evident correlation to gender but with a negative correlation to donor age (r_s = -0.550, p = 0.012). Accordingly, MSC capable to form bone (Fig. 1A) were derived from significantly younger donors (mean age 29.6, SEM ±4.08, p = 0.012) compared to MSC which failed

Table 1. Donor characteristics and MSC *in vitro* parameters in relation to bone formation listed by increasing generation time.

Donor	Age	Gender	Ectopic bone formation	Generation time* [h]	Days in culture	Max. ALP activity** [ng substrate/µg protein]/min	Max. calcification** [µg calcium/µg protein]
1	19	m	yes	27.38	16	8.27	28.50
2	42	m	yes	29.40	17	4.85	23.08
3	23	f	yes	29.81	16	16.90	73.11
4'	41	m	yes	30.28	12	13.87	17.02
5	14	m	yes	30.48	15	10.04	14.47
6	19	m	yes	33.86	14	23.56	5.51
7	26	f	yes	33.99	17	3.75	37.05
8	30	m	yes	36.00	17	9.30	10.07
9	24	f	yes	42.94	14	5.90	15.33

10	61	f	no	43.52	18	1.04	46.33
11'	61	m	yes	48.26	19	2.33	16.57
12	56	m	no	48.88	19	0.56	42.47
13'	27	f	yes	55.38	18	4.41	19.54
14	43	m	no	62.37	19	1.08	24.80
15	41	f	no	62.74	19	0.43	22.56
16	56	m	no	66.77	26	0.79	31.62
17	11	f	no	101.46	25	0.75	26.36
18	46	f	no	104.64	19	1.65	12.69
19'	74	f	no	107.49	18	2.93	23.35
20	74	m	no	189.62	25	0.24	44.38

*at time point of implantation, **during osteogenic *in vitro* differentiation, ' = not included in gene expression analysis since used for experiments in Table 2, -------------- optimal threshold (43.23 h/PD).
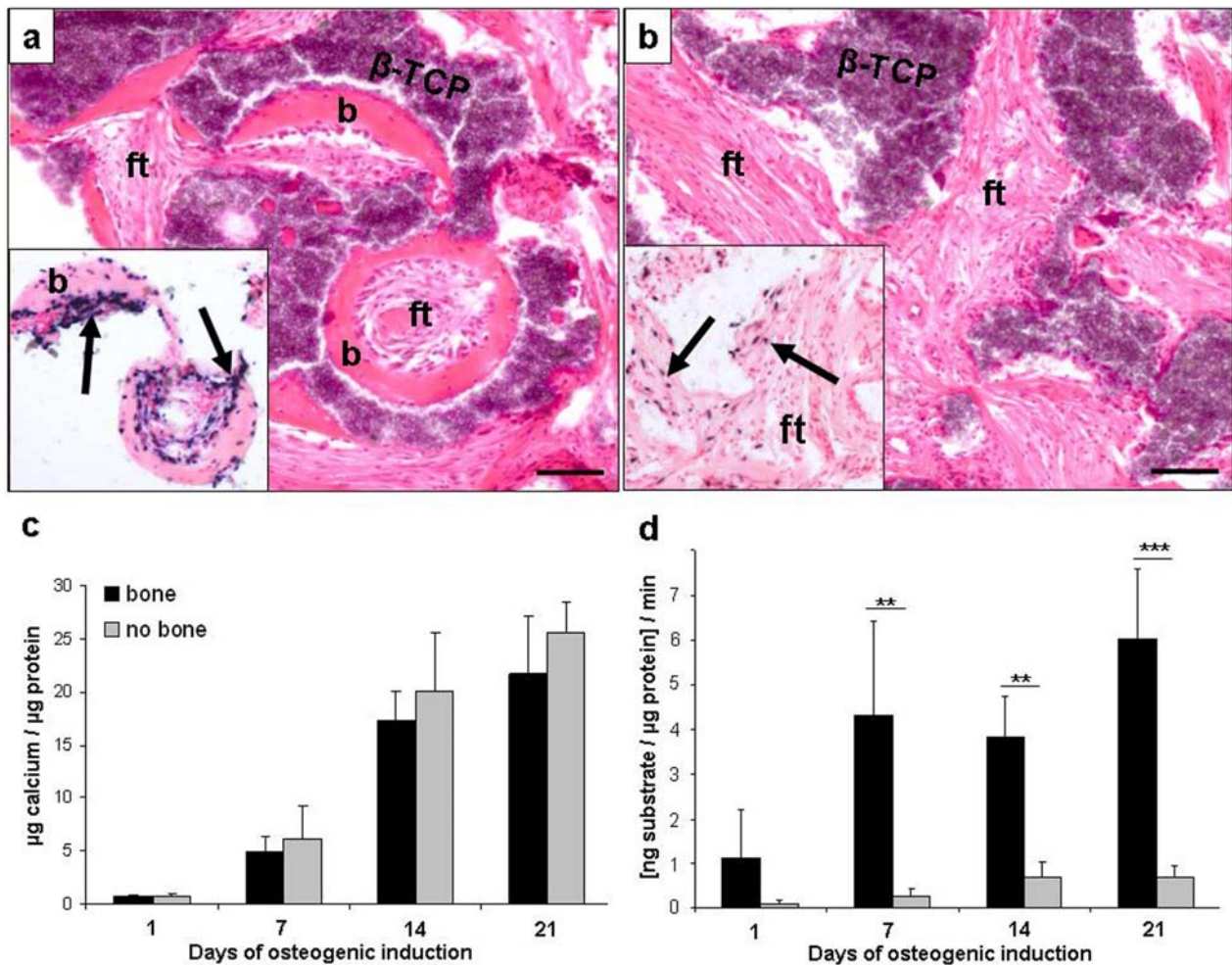
Fig. 1. The standard osteogenic *in vitro* mineralisation assay does not correlate with *in vivo* bone formation. (**a-b**) Representative pictures of H&E-stained histological sections of β-TCP/MSC explants with (**a**) and without (**b**) bone formation. Human-specific Alu *in situ* hybridisation revealed human origin of bone forming cells (**a**, inset, arrows) and only few human cells within the fibrous tissue of explants without bone formation (**b**, inset, arrows). (**c**) Alizarin red S-stained calcium-deposition during 21 d of osteogenic *in vitro* differentiation. All MSC populations were able to deposit a calcium-rich extracellular matrix *in vitro*, independent of their bone forming ability *in vivo*. (**d**) ALP activity in cell lysates was measured during osteogenic monolayer differentiation on day 7 (**$p = 0.004$), 14 (**$p = 0.002$) and 21 (***$p = 0.001$) of induction. MSC which formed bone *in vivo* showed significantly higher ALP activity during 21 d of osteogenic *in vitro* induction. b = heterotopic bone, ft = fibrous tissue. Scale bar: 100 μm. Error bars represent standard error of the mean.

in bone formation (Fig. 1B) (mean age 51.3, SEM ±6.45, Table 1). Osteoblast-like cells depositing bone in the pores of the β-TCP granules were of human origin (Fig. 1A, inset). Only few or no human cells were identified within the fibrous tissue of β-TCP/MSC constructs from the non-bone forming group (Fig. 1B, inset). This indicated that MSC which were incapable to form bone migrated away from the constructs or died. Vascular structures were apparent in all constructs independent of bone formation. MSC-free β-TCP granules or carrier-free MSC never revealed bone structures (data not shown). There was no correlation between the site of bone marrow harvest or the pathology of donors, like osteoarthritis or other diseases, and the bone forming potency of the MSC.

Correlation of *in vitro* osteogenesis with *in vivo* bone formation

In parallel to transplantation, MSC populations of 20 donors were subjected to osteogenic *in vitro* conditions for 21 days in culture. Osteogenesis resulted in a time-dependent increase of ALP activity and calcium deposition for all donor MSC. Mineralisation was not significantly different between MSC groups with or without bone formation ($p \leq 0.112$) (Fig. 1C).

ALP activity revealed a high donor variability during osteogenic *in vitro* induction with bone-forming MSC populations reaching significantly higher ALP values at day 7 ($p = 0.004$), day 14 ($p = 0.002$) and day 21 ($p = 0.001$) (Fig. 1D). Thus, a strong positive correlation (r_s
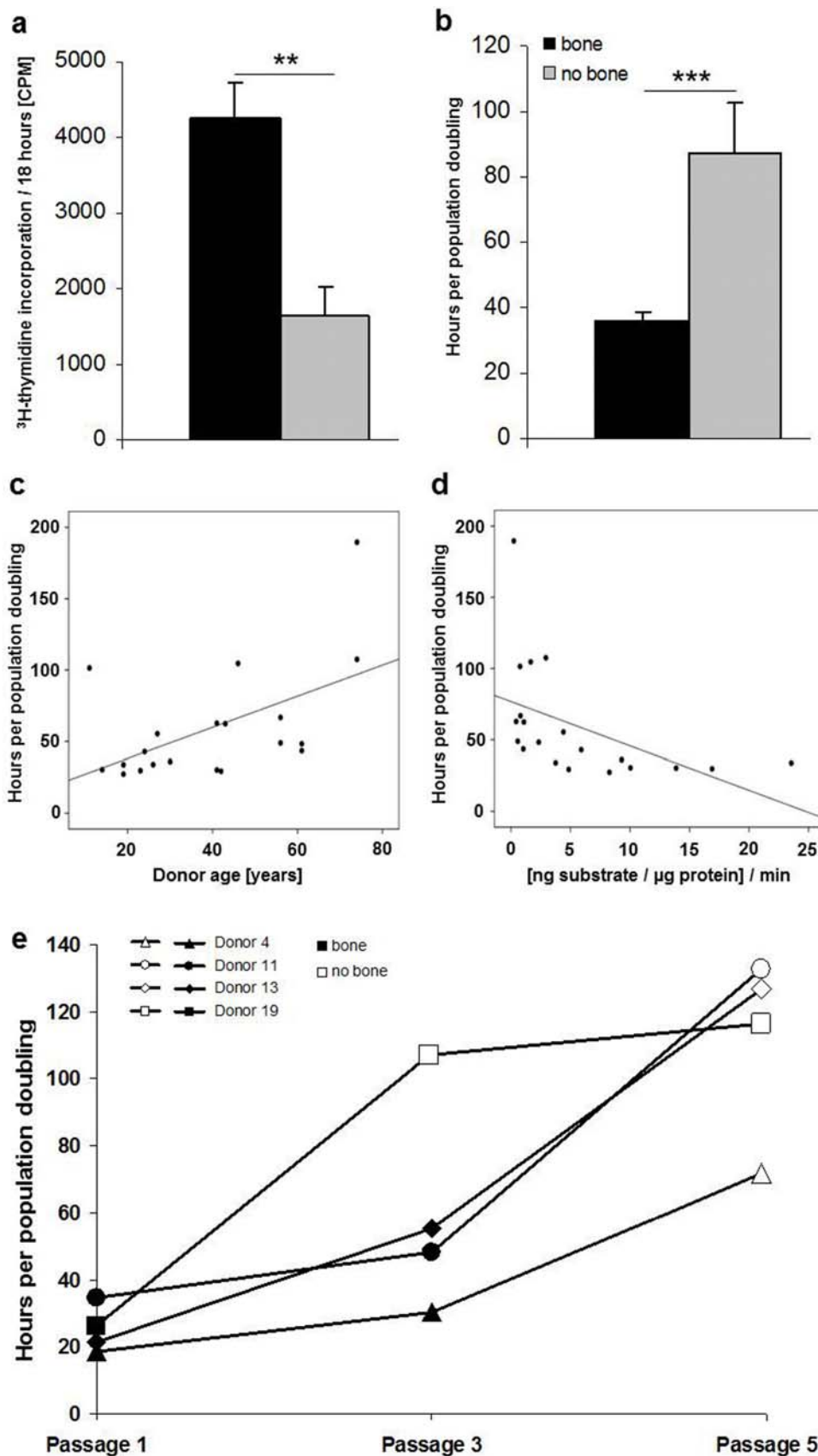
Fig. 2. Growth characteristics of undifferentiated MSC prior to transplantation. (**a**) Bone forming MSC populations incorporated significantly more ^{3}H-thymidine (**p = 0.002) within 18 h *in vitro* and (**b**) revealed a significantly shorter (***p ≤ 0.001) generation time than MSC without the ability to form bone. Bars represent standard error of the mean. (**c**) Generation time of expanded MSC correlated positively with donor age (r_p = 0.529, *p* = 0.016) and (**d**) negatively (r_p = -0.694, *p* ≤ 0.001) with the maximum ALP activity during osteogenic *in vitro* differentiation. (**e**) Increased doubling time correlated with loss of bone formation during serial passaging of MSC.

Table 2. Generation time and maximum ALP activity of MSC during serial passaging (P1-P5).

Donor	Generation time* [h]			Max. ALP activity** [ng substrate/µg protein]/min		
	P1	P3	P5	P1	P3	P5
4	**18.57**	**20.28**	72.17	**15.54**	**13.87**	21.89
11	**34.71**	**48.26**	133.14	**6.49**	**2.33**	10.40
13	**21.22**	**55.38**	127.09	**10.00**	**4.41**	13.84
19	**26.35**	107.49	116.80	**7.75**	2.93	8.31

*At time point of implantation, **During osteogenic *in vitro* differentiation, bold = samples that showed bone formation *in vivo.*

Table 3. Generation time and time in culture of MSC expanded under standard versus enriched culture conditions.

Donor	Age	Gender	Expansion medium Generation time* [h]	Conditioned ES medium Generation time* [h]	Days in culture
21	23	f	46.13	**38.96**	13
22	46	m	50.88	**34.40**	16
23	64	f	**59.45**	**32.57**	11
24	36	f	65.87	**39.08**	18
25	84	m	68.85	**40.25**	13

*At time point of implantation, bold = samples that showed bone formation *in vivo.*

= 0.845, $p \leq 0.001$) existed between bone formation and *in vitro* ALP induction after osteogenic stimulation. ROC analysis was applied in order to determine an optimal ALP threshold level which would best predict bone formation in our model. The optimal decision threshold for peak ALP values was 3.34 ng substrate/minute and µg protein. All MSC populations with values below this cut-off level failed to form bone (100.0 % specificity), while all bone forming samples except one (donor 11, Table 1), had maximal ALP values above this threshold, corresponding to a test sensitivity of 90.9 %.

Correlation of growth rate with bone formation
In contrast to the outcome of an *in vitro* osteogenic assay, growth parameters are known before transplantation of MSC and are, thus, attractive as possible predictors of bone formation capacity in a clinical setting. MSC samples forming bone revealed a significantly higher ³H-thymidine incorporation into DNA (2.58-fold, $p = 0.002$) (Fig. 2A) and thus a higher proliferation rate than MSC incapable to form bone. Bone forming MSC had a significantly shorter mean generation time (36.16 h per population doubling (h/PD), SEM ±2.7, $p \leq 0.001$) than MSC without bone formation (87.49 h/PD, SEM ±15.1) (Fig. 2B) revealing a strong correlation between generation time and bone formation ($r_s = -0.810$, $p \leq 0.001$). The optimal decision level for prediction of bone formation based on generation time was 43.23 h/PD according to ROC analysis (dashed line, Table 1). All MSC failing to form bone grew more slowly than this threshold (100 % specificity) while all but 2 donor populations forming bone were faster than

this threshold (donor 11 and 13, Table 1) yielding a test sensitivity of 81.8 %. Thus, at the chosen conditions, doubling time at the day of transplantation would have correctly predicted *in vivo* bone formation capability of 18 out of 20 donors without any false positives.

Since faster growing MSC populations reached P3 earlier than cells growing more slowly, bone forming MSC were transplanted after a significantly shorter time in culture (mean 15.91 days, SEM ±0.61) than MSC of the other group (20.89 days, SEM ±1.12, $p \leq 0.001$). All MSC cultured for 17 days or less formed bone (Table 1) while MSC expanded for more than 19 days never formed bone under our expansion conditions. Age and ALP activity correlated significantly with the proliferation rate of MSC (Fig. 2C-D) demonstrating that these parameters represent no independent determinants of bone forming ability.

Serial passaging and *in vivo* bone formation
We next challenged the determined decision levels for ALP-based and proliferation-based prediction by testing the bone forming ability of four MSC populations during serial passaging (Table 2). Generation time of each MSC population increased with every passage and bone formation capacity declined in parallel. While all P1 cells formed ectopic bone (Fig. 2E, closed symbols), one MSC population had lost its bone formation ability at P3 while at P5 all four MSC populations were negative (Fig. 2E, open symbols). The generation time of about 43 h/PD extracted before, again, correctly predicted bone formation for 10 out of these 12 transplanted MSC populations (P1, P3, P5 from four donors each) with no false positive results.
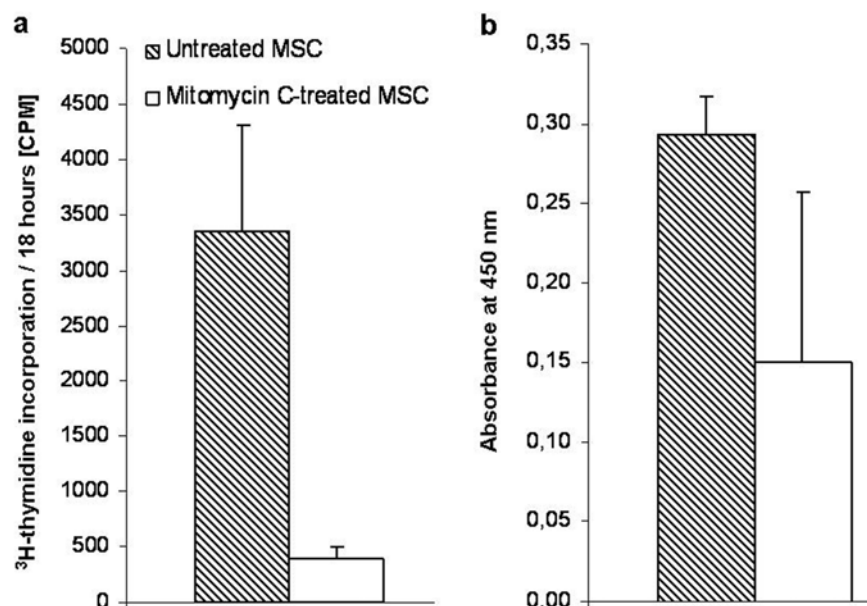
Fig. 3. Arrest of cell proliferation by mitomycin C. (**a**) DNA synthesis dropped to 12 % by mitomycin C-treatment (white bar) compared to MSC cultivated in the expansion medium (striped bar, n = 4). (**b**) Cell metabolism assessed by a WST-1 assay was reduced by half in mitomycin C-treated MSC compared to untreated controls (n = 2). Bars represent standard error of the mean.

Prediction based on *in vitro* ALP activity, however, did not pass this test. Although ALP activity was high in all P1 populations and decreased at P3, it increased again at P5 reaching the highest values for cells without bone forming ability (Table 2). Thus, in contrast to generation time, the *in vitro* ALP response to osteogenic induction turned out to be no robust predictor of heterotopic bone formation.

Modulation of proliferation rate can rescue *in vivo* bone formation

In order to look for a causal relationship between mitotic activity and heterotopic bone formation capacity, we tried to rescue inferior MSC populations by improved expansion under enhanced conditions. Slower *versus* faster growing MSC were produced from the same marrow aspirates by expansion in culture medium versus enriched conditions adapted from embryonal stem (ES) cell protocols (donor 21-25, Table 3). MSC in ES-medium incorporated on average 8.5-fold more ^{3}H-thymidine (not shown) and revealed 1.58-fold shorter generation times (Table 3) compared to MSC under standard expansion. At the same time point (near confluence at P2, day 11-18, depending on the donor) both MSC populations from each donor were harvested and transplanted. While all ES-medium expanded MSC grew faster than 43 h/PD and formed heterotopic bone, the corresponding standard cultures remained above 43 h/PD and 4 of these 5 MSC populations could not form bone as predicted according to generation time. Altogether this demonstrated that enhancing the proliferation rate rescued bone formation of inferior MSC suggesting a causal relationship between proliferation rate and *in vivo* bone formation.

No bone formation without proliferation

To decide whether growth is a prerequisite for bone formation, human MSC (donor 26-29, aged 17-79 years) with a permissive generation time at P2 were treated for 2 h with the mitotic inhibitor mitomycin C which irreversibly blocks DNA synthesis and inhibits proliferation. DNA synthesis dropped to 12 % by this treatment within 18 h (Fig. 3A, n = 4 donors) while values for cell metabolism were reduced by half (Fig. 3B, n = 2 donors), demonstrating that mitomycin C-treated cells were alive but unable to proliferate. After ectopic transplantation of constructs consisting of 10 mg β-TCP and either treated or untreated MSC (1x 10^6 cells, P2), respectively, none of the mitomycin C-treated MSC formed bone, while the corresponding untreated MSC (generation times 21.89 to 34.43 h/PD) all formed bone. During osteogenic *in vitro* induction, however, all mitomycin C-treated cells were able to deposit a mineralised matrix (data not shown).

Molecular correlates of *in vivo* bone formation

In order to extract molecular markers as potential predictors, gene expression profiling was performed for 16 MSC populations from Table 1, half of which had shown bone formation capability in P3. Cluster analysis identified a group of 4 closely related MSC populations which had formed bone and 3 closely related MSC populations which did not form bone. Gene signatures of these two groups differed by 311 genes at significance level. When this selection of genes was used for clustering of all 16 samples (Fig. 4A) two groups of 8 samples each were obtained in which all bone forming MSC were separated from all non-bone forming cells except one wrong sample in each group.

Of the 311 differentially expressed genes, 230 were higher expressed in bone-forming MSC (1.8-fold to 34.9-fold) including many cell cycle-associated genes like CDC20, CDCA7, CDC45, CDCA5 and the cyclins CCNB2, CCNA2, CCNE2, CCNF associated with cell proliferation (Table 4). Functional annotation of these genes by the DAVID program (Dennis *et al.*, 2003; Huang *et al.*, 2009) revealed mitosis, cell division, DNA replication and related pathways as main biological functions.

In the group of MSC that did not form bone, 81 genes were higher expressed. These included genes of the histone clusters HIST1H1C, HIST1H4H, HIST2H2AC, HIST2H2AA3, and molecules relevant for the formation of nucleosomes, dense chromatin, or capable of protein-DNA-complex formation. Some genes were associated with apoptosis (Table 5). Selected transcripts were confirmed by RT-PCR to have a significantly different expression level between the bone and not bone forming group (Fig. 4B). In summary, molecular analysis corroborated cell growth and an open chromatin as main determinant of *in vivo* bone formation making further investigation into molecular prediction assays promising.

Discussion

We here present a strategy to predict the heterotopic bone forming ability of human MSC populations in a β-TCP scaffold by a surprisingly simple potency test relying on determination of the generation time of MSC at the time of transplantation. Our study, for the first time, establishes a causal relationship between proliferation ability and heterotopic *in vivo* bone formation potency of human MSC and identifies a rate limiting proliferative activity as crucial for the success of neo-bone formation. A threshold set for generation time (43.23 h) at the time of MSC transplantation allowed, at our expansion conditions, to correctly predict the *in vivo* outcome of more than 20 donor populations with high specificity and sensitivity. This threshold proved also valuable when MSC were expanded for different passages and under altered expansion conditions. Proliferation rate also predicted the loss of heterotopic bone formation with increasing passage seen here in agreement with a recent study (Agata *et al.*, 2010) suggesting that time in culture is an alternate growth-dependent parameter of bone formation. Overwhelming molecular evidence from genome-wide transcriptome analysis confirmed growth and an open chromatin status as the major functional correlates of heterotopic bone formation. Altogether our data suggest that, in order to be successful, MSC have to be transplanted in a time window in which sufficient cells show high anabolism as major prerequisites for trophic and osteogenic activity at the site of transplantation. Beside its simplicity, a sensitivity of about 80 % at a specificity of 100 % under our conditions makes this assay quite attractive in the context of clinical use.

Why is growth such a dominant parameter in a heterotopic osteogenic differentiation model where osteoinductive growth factors, appropriate mechanical
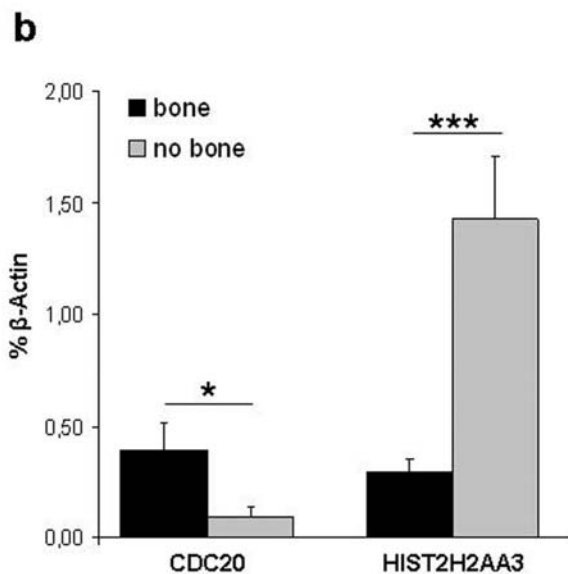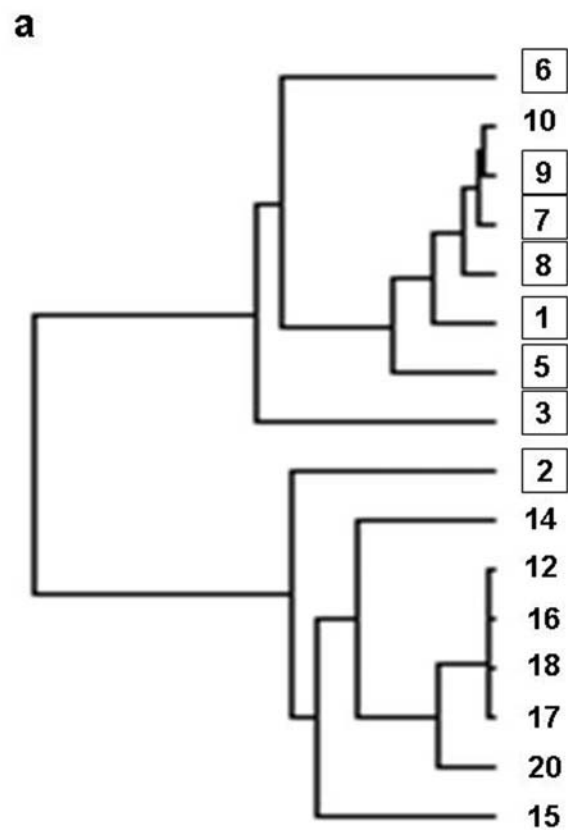
Fig. 4. Gene expression analysis of expanded MSC at the time point of transplantation. Genome wide expression analysis was carried out for MSC populations of 16 donors. (**a**) Cluster analysis based on 311 genes of MSC populations with (numbers in boxes) and without the ability to form ectopic bone *in vivo*. (**b**) Real-time PCR analysis confirmed the expression differences of two selected genes obtained by the array analysis. CDC20 was higher expressed (*p = 0.015) in the bone forming group, whereas HIST2H2AA3 was higher (*p = 0.001) in the MSC group without bone formation. Bars represent standard error of the mean.

Table 4a. Genes with significantly higher expression in expanded MSC capable to form bone after subcutaneous transplantation in SCID mice (part 1).

Gene symbol	Gene name	Fold change to non-bone forming MSC populations	Reference
CDC20	CDC20 cell division cycle 20 homolog	34.95	NM_001255.1
UBE2C	Ubiquitin-conjugating enzyme E2C	23.93	NM_181800.1
PRC1	Protein regulator of cytokinesis 1	23.09	NM_003981.2
TOP2A	Topoisomerase (DNA) II alpha 170kDa	19.87	NM_001067.2
KIAA0101	KIAA0101 (KIAA0101), transcript variant 1	18.43	NM_014736.4
KIF20A	Kinesin family member 20A	16.84	NM_005733.1
CCNB2	Cyclin B2	16.13	NM_004701.2
TYMS	Thymidylate synthetase	14.58	NM_001071.1
NUSAP1	Nucleolar and spindle associated protein 1	14.38	NM_016359.2
PTTG1	Pituitary tumor-transforming 1	12.91	NM_004219.2
CCNA2	Cyclin A2	12.80	NM_001237.2
BIRC5	Baculoviral IAP repeat-containing 5 (survivin)	12.78	NM_001168.2
KIFC1	Kinesin family member C1	12.72	NM_002263.2
Pfs2	GINS complex subunit 2	12.39	NM_016095.1
UBE2C	Ubiquitin-conjugating enzyme E2C	12.23	NM_181803.1
CDCA7	Cell division cycle associated 7	11.74	NM_145810.1
CDC45L	CDC45 cell division cycle 45-like	11.23	NM_003504.3
CDCA5	Cell division cycle associated 5	10.71	NM_080668.2
HMMR	Hyaluronan-mediated motility receptor	10.61	NM_012485.1
CDKN3	Cyclin-dependent kinase inhibitor 3	10.58	NM_005192.2
TK1	Thymidine kinase 1	10.57	NM_003258.1
AURKB	Aurora kinase B	10.28	NM_004217.1
ASPM	Asp (abnormal spindle)-like, microcephaly associated	10.27	NM_018136.2
OIP5	Opa interacting protein 5	10.13	NM_007280.1
TRIP13	Thyroid hormone receptor interactor 13	10.04	NM_004237.2
MCM7	Minichromosome maintenance complex component 7	9.87	NM_182776.1
FLJ40629	Cytoskeleton associated protein 2-like	9.83	NM_152515.2
CEP55	Centrosomal protein 55kDa	9.77	NM_018131.3
PBK	PDZ binding kinase	9.50	NM_018492.2
RRM2	Ribonucleotide reductase M2 polypeptide	9.44	NM_001034.1
STMN1	Stathmin 1/oncoprotein 18	9.12	NM_005563.3
HCAP-G	Non-SMC condensin I complex, subunit G	8.70	NM_022346.3
HIST1H4C	Histone cluster 1	8.61	NM_003542.3
CENPM	Centromere protein M	8.61	NM_001002876.1
AURKA	Aurora kinase A	8.53	NM_198434.1
PLK4	Polo-like kinase 4	8.41	NM_014264.2
AURKA	Aurora kinase A	8.38	NM_198434.1
CENPA	Centromere protein A, 17kDa	7.99	NM_001809.2
DLG7	Discs, large homolog 7	7.92	NM_014750.3
CDCA8	Cell division cycle associated 8	7.83	NM_018101.2
TPX2	TPX2, microtubule-associated, homolog	7.60	NM_012112.4
C20orf129	Chromosome 20 open reading frame 129	7.45	NM_030919.1
RAD51AP1	RAD51 associated protein 1	7.18	NM_006479.2
TTK	TTK protein kinase	6.99	NM_003318.3
MCM5	MCM5 minichromosome maintenance deficient 5, cell division cycle 46	6.97	NM_006739.2
MCM4	MCM4 minichromosome maintenance deficient 4	6.95	NM_005914.2
LMNB1	Lamin B1	6.41	NM_005573.2
MPHOSPH1	M-phase phosphoprotein 1	6.39	NM_016195.2

Table 4b. Genes with significantly higher expression in expanded MSC capable to form bone after subcutaneous transplantation in SCID mice (continued – part 2).

BUB1	BUB1 budding uninhibited by benzimidazoles 1	6.35	NM_004336.2
SPC24	SPC24, NDC80 kinetochore complex component	6.19	NM_182513.1
FANCD2	Fanconi anemia, complementation group D2	5.91	NM_001018115.1
MCM7	Minichromosome maintenance complex component 7	5.80	NM_005916.3
MCM3	MCM3 minichromosome maintenance deficient 3	5.69	NM_002388.3
ANLN	Anillin, actin binding protein	5.66	NM_018685.2
FKSG14	Leucine zipper protein FKSG14	5.57	NM_022145.2
KIF2C	Kinesin family member 2C	5.56	NM_006845.2
NCAPG2	Non-SMC condensin II complex, subunit G2	5.52	NM_017760.5
PRR11	Proline rich 11 (PRR11), mRNA.	5.51	NM_018304.1
POLE2	Polymerase (DNA directed), epsilon 2 (p59 subunit)	5.45	NM_002692.2
CDC2	Cell division cycle 2, G1 to S and G2 to M	5.43	NM_033379.2
MCM2	MCM2 minichromosome maintenance deficient 2, mitotin	5.41	NM_004526.2
C16orf60	Centromere protein N	5.39	NM_018455.3
FOXM1	Forkhead box M1	5.37	NM_021953.2
DKFZp762E1312	Hypothetical protein DKFZp762E1312	5.32	NM_018410.2
APOBEC3B	Apolipoprotein B mRNA editing enzyme, catalytic polypeptide-like 3B	5.25	NM_004900.3
FEN1	Flap structure-specific endonuclease 1	5.22	NM_004111.4
MELK	Maternal embryonic leucine zipper kinase	5.21	NM_014791.2
EXO1	Exonuclease 1	5.18	NM_003686.3
SOCS2	Suppressor of cytokine signaling 2	5.11	NM_003877.3
CENPF	Centromere protein F, 350/400ka	4.99	NM_016343.3
UBE2T	Ubiquitin-conjugating enzyme E2T	4.97	NM_014176.1
C22orf18	Centromere protein M	4.94	NM_024053.3
CDK2	Cyclin-dependent kinase 2	4.89	NM_001798.2
PRIM1	Primase, polypeptide 1, 49kDa	4.86	NM_000946.2
RFC4	Replication factor C (activator 1) 4, 37kDa	4.84	NM_002916.3
KIF4A	Kinesin family member 4A	4.83	NM_012310.2
TMPO	Thymopoietin	4.80	NM_003276.1
FLJ25416	Chromosome 11 open reading frame 82	4.77	NM_145018.2
RPL39L	Ribosomal protein L39-like	4.76	NM_052969.1
RRM1	Ribonucleotide reductase M1 polypeptide	4.75	NM_001033.2
RACGAP1	Rac GTPase activating protein 1	4.67	NM_013277.2
DNAJC9	DnaJ (Hsp40) homolog, subfamily C, member 9	4.58	NM_015190.3
POLQ	Polymerase (DNA directed), theta	4.56	NM_199420.2
GTSE1	G-2 and S-phase expressed 1	4.55	NM_016426.4
CDT1	Chromatin licensing and DNA replication factor 1	4.55	NM_030928.2
HAS2	Hyaluronan synthase 2	4.52	NM_005328.1
RFC3	Replication factor C (activator 1) 3, 38kDa	4.50	NM_181558.1
SMC4	Structural maintenance of chromosomes 4	4.48	NM_001002800.1
WDR51A	WD repeat domain 51A	4.44	NM_015426.2
CCNE2	Cyclin E2	4.38	NM_057735.1
TROAP	Trophinin associated protein (tastin)	4.37	NM_005480.2
MCM6	MCM6 minichromosome maintenance deficient 6	4.33	NM_005915.4
ATAD2	ATPase family, AAA domain containing 2	4.33	NM_014109.2
CENPM	Centromere protein M	4.26	NM_001002876.1
CKS1B	CDC28 protein kinase regulatory subunit 1B	4.21	NM_001826.1
CCNF	Cyclin F	4.15	NM_001761.1

Table 4c. Genes with significantly higher expression in expanded MSC capable to form bone after subcutaneous transplantation in SCID mice (continued – part 3).

KIF23	Kinesin family member 23	4.15	NM_004856.4
CDCA3	Cell division cycle associated 3	4.05	NM_031299.3
RFC5	Replication factor C (activator 1) 5	4.05	NM_007370.3
KIF14	Kinesin family member 14	3.95	NM_014875.1
SUV39H1	Suppressor of variegation 3-9 homolog 1	3.95	NM_003173.1
H2AFZ	H2A histone family, member Z	3.93	NM_002106.3
MCM10	Minichromosome maintenance complex component 10	3.88	NM_018518.3
HMMR	Hyaluronan-mediated motility receptor	3.80	NM_012484.1
DDX39	DEAD (Asp-Glu-Ala-Asp) box polypeptide 39	3.79	NM_005804.2
CENPA	Centromere protein A	3.78	NM_001042426.1
NUDT1	Nudix (nucleoside diphosphate linked moiety X)-type motif 1	3.73	NM_198948.1
CHAF1B	Chromatin assembly factor 1, subunit B (p60)	3.71	NM_005441.2
RFC3	Replication factor C (activator 1) 3, 38kDa	3.64	NM_002915.2
DNMT1	DNA (cytosine-5-)-methyltransferase 1	3.64	NM_001379.1
C6orf173	Chromosome 6 open reading frame 173	3.60	NM_001012507.1
FLJ20364	Hypothetical protein FLJ20364	3.59	NM_017785.2
MCM4	Minichromosome maintenance complex component 4	3.56	NM_182746.1
PLK1	Polo-like kinase 1	3.52	NM_005030.3
TIMELESS	Timeless homolog	3.52	NM_003920.2
PSRC1	Proline/serine-rich coiled-coil 1	3.51	NM_001005290.2
PAQR4	Progestin and adipoQ receptor family member IV	3.47	NM_152341.2
HNRPA1	Heterogeneous nuclear ribonucleoprotein A1	3.42	NM_002136.1
BARD1	BRCA1 associated RING domain 1	3.39	NM_000465.1
KIAA0101	KIAA0101	3.36	NM_014736.4
RFC4	Replication factor C (activator 1) 4, 37kDa	3.33	NM_002916.3
SGOL1	Shugoshin-like 1	3.30	NM_001012413.1
SKP2	S-phase kinase-associated protein 2 (p45)	3.30	NM_032637.2
CCDC34	Coiled-coil domain containing 34	3.29	NM_030771.1
CHEK1	CHK1 checkpoint homolog	3.24	NM_001274.2
CDC25A	Cell division cycle 25A	3.24	NM_001789.2
GPSM2	G-protein signalling modulator 2	3.22	NM_013296.3
ZWILCH	Zwilch, kinetochore associated, homolog	3.20	NR_003105.1
EZH2	Enhancer of zeste homolog 2	3.19	NM_152998.1
CNAP1	Non-SMC condensin I complex, subunit D2	3.18	NM_014865.2
EZH2	Enhancer of zeste homolog 2	3.17	NM_004456.3
RPA3	Replication protein A3, 14kDa	3.17	NM_002947.3
RBMX	RNA binding motif protein, X-linked	3.15	NM_002139.2
LIG1	Ligase I, DNA, ATP-dependent	3.15	NM_000234.1
BIRC5	Baculoviral IAP repeat-containing 5 (survivin)	3.13	NM_001012271.1
CACYBP	Calcyclin binding protein	3.11	NM_014412.2
FUS	Fusion (involved in t(12;16) in malignant liposarcoma)	3.09	NM_004960.2
NUSAP1	Nucleolar and spindle associated protein 1	3.07	NM_018454.5
LBR	Lamin B receptor	3.06	NM_002296.2
TACC3	Transforming, acidic coiled-coil containing protein 3	3.05	NM_006342.1
C18orf24	Chromosome 18 open reading frame 24	3.05	NM_145060.1
PPIL5	Peptidylprolyl isomerase (cyclophilin)-like 5	3.04	NM_152329.3
HNRPA2B1	Heterogeneous nuclear ribonucleoprotein A2/B1	3.03	NM_031243.1
ASF1B	ASF1 anti-silencing function 1 homolog B	3.02	NM_018154.2

Table 4d. Genes with significantly higher expression in expanded MSC capable to form bone after subcutaneous transplantation in SCID mice (continued – part 4).

POLA2	Polymerase (DNA directed), alpha 2 (70kD subunit)	3.02	NM_002689.2
ILF3	Interleukin enhancer binding factor 3, 90kDa	2.99	NM_004516.2
BCL2L12	BCL2-like 12 (proline rich)	2.98	NM_052842.2
RNASEH2A	Ribonuclease H2, subunit A	2.95	NM_006397.2
C17orf53	Chromosome 17 open reading frame 53	2.93	NM_024032.2
KIF15	Kinesin family member 15	2.93	NM_020242.1
FOXM1	Forkhead box M1	2.92	NM_202002.1
BCL2L12	BCL2-like 12 (proline rich)	2.91	NM_001040668.1
TFAM	Transcription factor A, mitochondrial	2.89	NM_003201.1
EXOSC9	Exosome component 9	2.83	NM_005033.1
E2F2	E2F transcription factor 2	2.82	NM_004091.2
MNS1	Meiosis-specific nuclear structural 1	2.78	NM_018365.1
FLJ13912	GINS complex subunit 3	2.75	NM_022770.2
CDC25C	Cell division cycle 25 homolog C	2.73	NM_001790.3
DIAPH3	Diaphanous homolog 3	2.72	NM_001042517.1
SLC25A15	Solute carrier family 25 (mitochondrial carrier; ornithine transporter) member 15	2.72	NM_014252.2
SNRPB	Small nuclear ribonucleoprotein polypeptides B and B1	2.71	NM_003091.3
MCM10	Minichromosome maintenance complex component 10	2.70	NM_018518.3
FLJ13909	Hypothetical protein FLJ13909	2.63	NM_025108.1
BLM	Bloom syndrome	2.58	NM_000057.1
POLA1	Polymerase (DNA directed), alpha 1	2.56	NM_016937.2
LSM2	LSM2 homolog, U6 small nuclear RNA associated	2.56	NM_021177.3
GEMIN6	Gem (nuclear organelle) associated protein 6	2.55	NM_024775.9
EIF2B2	Eukaryotic translation initiation factor 2B, subunit 2 beta, 39kDa	2.54	NM_014239.2
FLJ22624	FLJ22624 protein	2.53	NM_024808.2
CBX5	Chromobox homolog 5	2.52	NM_012117.1
SNRPB	Small nuclear ribonucleoprotein polypeptides B and B1	2.50	NM_003091.3
CDC25C	Cell division cycle 25 homolog C	2.49	NM_001790.3
HNRPM	Heterogeneous nuclear ribonucleoprotein M	2.47	NM_031203.1
C2orf32	Chromosome 2 open reading frame 32	2.46	NM_015463.1
LMNB2	Lamin B2	2.45	NM_032737.2
CGGBP1	CGG triplet repeat binding protein 1	2.45	NM_003663.3
DKFZP564J0863	DKFZP564J0863 protein	2.44	NM_015459.3
GALE	UDP-galactose-4-epimerase	2.44	NM_000403.3
SLD5	GINS complex subunit 4	2.43	NM_032336.1
NPM3	Nucleophosmin/nucleoplasmin, 3	2.43	NM_006993.1
CSE1L	CSE1 chromosome segregation 1-like	2.42	NM_001316.2
SMC2L1	SMC2 structural maintenance of chromosomes 2-like 1	2.39	NM_006444.1
PFAS	Phosphoribosylformylglycinamidine synthase	2.38	NM_012393.1
EXOSC2	Exosome component 2	2.37	NM_014285.4
TUBB2C	Tubulin, beta 2C	2.36	NM_006088.5
INCENP	Inner centromere protein antigens 135/155kDa	2.36	NM_001040694.1
SNRPA	Small nuclear ribonucleoprotein polypeptide A	2.34	NM_004596.3
CDK2	Cyclin-dependent kinase 2	2.34	NM_001798.2
C16orf61	Chromosome 16 open reading frame 61	2.34	NM_020188.2
RPS7	Ribosomal protein S7	2.33	NM_001011.3
PDSS1	Prenyl (decaprenyl) diphosphate synthase, subunit 1	2.33	NM_014317.3
SAAL1	Serum amyloid A-like 1	2.32	NM_138421.1

Table 4e. Genes with significantly higher expression in expanded MSC capable to form bone after subcutaneous transplantation in SCID mice (continued – part 5).

MRPL35	Mitochondrial ribosomal protein L35	2.32	NM_145644.1
SNRPF	Small nuclear ribonucleoprotein polypeptide F	2.31	NM_003095.2
XTP3TPA	XTP3-transactivated protein A	2.29	NM_024096.1
NUP37	Nucleoporin 37kDa	2.28	NM_024057.2
C18orf55	Chromosome 18 open reading frame 55	2.26	NM_014177.1
MRPL11	Mitochondrial ribosomal protein L11	2.25	NM_016050.2
MRPL39	Mitochondrial ribosomal protein L39	2.24	NM_017446.2
CCDC5	Coiled-coil domain containing 5	2.23	NM_138443.2
C1orf33	Chromosome 1 open reading frame 33.	2.20	NM_016183.2
MGC13170	Chromosome 19 open reading frame 48	2.19	NM_199249.1
SNRPG	Small nuclear ribonucleoprotein polypeptide G	2.19	NM_003096.2
RPL29	Ribosomal protein L29	2.19	NM_000992.2
STRA13	Stimulated by retinoic acid 13 homolog	2.18	NM_144998.2
EMG1	EMG1 nucleolar protein homolog	2.17	NM_006331.4
POLE3	Polymerase (DNA directed), epsilon 3 (p17 subunit)	2.17	NM_017443.3
MRRF	Mitochondrial ribosome recycling factor	2.16	NM_138777.2
SMS	Spermine synthase	2.12	NM_004595.2
TMEM97	Transmembrane protein 97	2.11	NM_014573.1
FLJ14668	Family with sequence similarity 136, member A	2.10	NM_032822.1
RPL36A	Ribosomal protein L36a	2.09	NM_021029.4
TUBA6	Tubulin, alpha 1c	2.08	NM_032704.2
SLC25A5	Solute carrier family 25 (mitochondrial carrier; adenine nucleotide translocator), member 5	2.07	NM_001152.1
STOML2	Stomatin (EPB72)-like 2	2.06	NM_013442.1
MRPS31	Mitochondrial ribosomal protein S31	2.05	NM_005830.2
CARKL	Carbohydrate kinase-like	2.05	NM_013276.2
HMBS	Hydroxymethylbilane synthase	2.03	NM_001024382.1
C9orf40	Chromosome 9 open reading frame 40	1.99	NM_017998.1
SUHW4	Suppressor of hairy wing homolog 4	1.98	NM_001002844.1
MRPL12	Mitochondrial ribosomal protein L12	1.98	NM_002949.2
NAT10	N-acetyltransferase 10	1.98	NM_024662.1
NXT1	NTF2-like export factor 1	1.97	NM_013248.2
BANF1	Barrier to autointegration factor 1	1.97	NM_003860.2
HPRT1	Hypoxanthine phosphoribosyltransferase 1	1.96	NM_000194.1
NUP85	Nucleoporin 85kDa	1.93	NM_024844.2
RFWD3	Ring finger and WD repeat domain 3	1.89	NM_018124.3
DUSP12	Dual specificity phosphatase 12	1.84	NM_007240.1
C20orf20	Chromosome 20 open reading frame 20	1.80	NM_018270.3
ADSL	Adenylosuccinate lyase	1.75	NM_000026.1

Table 5. Genes with significantly higher expression in expanded MSC which were not able to form bone after subcutaneous transplantation in SCID mice.

Gene symbol	Gene name	Fold change to bone forming MSC populations	Reference
CCPG1	Cell cycle progression 1	6.6	NM_004748.3
HIST2H2AA3	Histone cluster 2, H2aa3	6.4	NM_003516.2
RARRES3	Retinoic acid receptor responder (tazarotene induced) 3	5.3	NM_004585.2
HIST2H2AC	Histone cluster 2, H2ac	5.1	NM_003517.2
HIST1H4H	Histone cluster 1, H4h	4.7	NM_003543.3
SOD2	Superoxide dismutase 2, mitochondrial	4.7	NM_001024465.1
BIRC3	Baculoviral IAP repeat-containing 3	4.5	NM_001165.3
PALM	Paralemmin	4.5	NM_002579.1
HIST1H1C	Histone cluster 1, H1c	4.5	NM_005319.3
RGMB	RGM domain family, member B	4.4	NM_001012761.1
CFB	Complement factor B	4.1	NM_001710.4
CREG1	Cellular repressor of E1A-stimulated genes 1	4.0	NM_003851.2
MANBA	Mannosidase, beta A, lysosomal	3.9	NM_005908.2
DAB2	Disabled homolog 2	3.8	NM_001343.1
HIST2H2BE	Histone cluster 2, H2be	3.7	NM_003528.2
SERPINF1	Serpin peptidase inhibitor, clade F	3.7	NM_002615.4
GRN	Granulin	3.7	NM_002087.2
KIAA0746	KIAA0746 protein	3.5	NM_015187.1
MGC17330	Phosphoinositide-3-kinase interacting protein 1	3.5	NM_052880.3
LAMP2	Lysosomal-associated membrane protein 2	3.4	NM_002294.1
LY96	Lymphocyte antigen 96	3.3	NM_015364.2
NUDT14	Nudix (nucleoside diphosphate linked moiety X)-type motif 14	3.3	NM_177533.2
LRRC32	Leucine rich repeat containing 32	3.3	NM_005512.1
DCAMKL1	Doublecortin and CaM kinase-like 1	3.3	NM_004734.2
PPGB	Protective protein for beta-galactosidase	3.2	NM_000308.1
OPTN	Optineurin	3.2	NM_001008213.1
ACSL5	Acyl-CoA synthetase long-chain family member 5	3.1	NM_203379.1
TPP1	Tripeptidyl peptidase I	3.1	NM_000391.2
NBL1	Neuroblastoma, suppression of tumorigenicity 1	3.0	NM_005380.4
NFE2L1	Nuclear factor (erythroid-derived 2)-like 1	3.0	NM_003204.1
CEECAM1	Cerebral endothelial cell adhesion molecule 1	3.0	NM_016174.3
PGCP	Plasma glutamate carboxypeptidase	2.9	NM_016134.2
NPDC1	Neural proliferation, differentiation and control	2.9	NM_015392.2
CHPF	Chondroitin polymerizing factor	2.9	NM_024536.4
CD82	CD82 antigen	2.9	NM_002231.3
BIRC3	Baculoviral IAP repeat-containing 3	2.8	NM_182962.1
SELM	Selenoprotein M	2.8	NM_080430.2
CYB5R1	Cytochrome b5 reductase 1	2.8	NM_016243.2
SH3PXD2A	SH3 and PX domains 2A	2.8	NM_014631.2
LAMP2	Lysosomal-associated membrane protein 2	2.7	NM_002294.1
TRAK2	Trafficking protein, kinesin binding 2	2.7	NM_015049.1
UACA	Uveal autoantigen with coiled-coil domains and ankyrin repeats	2.7	NM_018003.2
SAP18	Sin3A-associated protein	2.7	NM_005870.3
URB	Coiled-coil domain containing 80	2.7	NM_199512.1
NXPH4	Neurexophilin 4	2.6	NM_007224.1
DDR2	Discoidin domain receptor family, member 2	2.5	NM_006182.2
SMPD1	Sphingomyelin phosphodiesterase 1, acid lysosomal	2.5	NM_001007593.1
ALDH2	Aldehyde dehydrogenase 2 family	2.5	NM_000690.2
CLIPR-59	CAP-GLY domain containing linker protein 3	2.5	NM_015526.1
WIPI2	WD repeat domain, phosphoinositide interacting 2	2.5	NM_016003.3
C20orf31	ER degradation enhancer, mannosidase alpha-like 2	2.5	NM_018217.1
RRAGB	Ras-related GTP binding B	2.5	NM_006064.3
GSN	Gelsolin	2.5	NM_198252.1
FUCA1	Fucosidase, alpha-L- 1, tissue	2.5	NM_000147.2
IGFBP2	Insulin-like growth factor binding protein 2	2.5	NM_000597.2
SERINC1	Serine incorporator 1	2.5	NM_020755.2
CFLAR	CASP8 and FADD-like apoptosis regulator	2.5	NM_003879.3
CCL26	Chemokine (C-C motif) ligand 26	2.4	NM_006072.4
C9orf111	Patatin-like phospholipase domain containing 7	2.4	NM_152286.2
GNPTG	N-acetylglucosamine-1-phosphate transferase, gamma subunit	2.4	NM_032520.3
MGC33692	Similar to RIKEN cDNA 1700027J05 gene	2.3	NM_001001794.1
LRP1	Low density lipoprotein-related protein 1	2.3	NM_002332.1
SIL1	SIL1 homolog, endoplasmic reticulum chaperone	2.3	NM_001037633.1
LENG4	Leukocyte receptor cluster	2.3	NM_024298.2
ABHD4	Abhydrolase domain containing 4	2.2	NM_022060.2
FLJ21127	Tectonic	2.2	NM_024549.3
PTPRM	Protein tyrosine phosphatase, receptor type	2.2	NM_002845.2
ALDH4A1	Aldehyde dehydrogenase 4 family, member A1	2.2	NM_170726.1
PLXNA3	Plexin A3	2.2	NM_017514.2
SLC39A11	Solute carrier family 39 (metal ion transporter), member 11	2.2	NM_139177.2
ORF1-FL49	Putative nuclear protein ORF1-FL49	2.2	NM_032412.2
SDF4	Stromal cell derived factor 4	2.2	NM_016547.1
LOC283537	Hypothetical protein LOC283537	2.2	NM_181785.1
TXNRD1	Thioredoxin reductase 1	2.1	NM_003330.2
TMEM16K	Transmembrane protein 16K	2.1	NM_018075.2
TNFRSF14	Tumor necrosis factor receptor superfamily, member 14	2.1	NM_003820.2
SIL1	SIL1 homolog, endoplasmic reticulum chaperone	2.1	NM_022464.3
NISCH	Nischarin	2.0	NM_007184.2
RTN3	Reticulon 3	2.0	NM_201430.1
LRPAP1	Low density lipoprotein receptor-related protein associated protein 1	2.0	NM_002337.1
NEK6	NIMA (never in mitosis gene a)-related kinase 6	1.9	NM_014397.3

stimuli and a supporting bone-environment did not exist? One explanation may be that, in the first place, a high anabolism is needed to create an active microenvironment at the site of transplantation which allows activation of local cells and attraction of blood vessels in order to satisfy the enhanced demand for nutrients and oxygen for building up new bone tissue. Only if this trophic action of MSC is successfully achieved, possibly through a high amount of secreted factors, sufficient cells survive, stay in place and do more than integrating at low efficiency into fibrous tissue deposited by invading mouse cells. A second crucial aspect of a high proliferation rate and anabolism may be related to the mesengenic activity of MSC. In order to cope with the new 3D conditions after transplantation and the differentiation into osteoblasts, regulatory gene regions that the cell has probably never used before, may need to be accessed. DNA condensing molecules like histones and nucleosome-forming molecules were significantly higher expressed in non-bone forming MSC having a generation time above 43 h and being in culture for longer than 18 days. This provides indirect evidence of a time window of more open chromatin up to this time point which may be crucial to allow cell adaptation including initiation of the *in vivo* osteogenic differentiation cascade. A third possibility to explain the important role of proliferation may be the need for high cell anabolism to create an environment allowing sufficient release of calcium-phosphate ions from the β-TCP scaffold. This could render the carrier more osteoinductive and may drive osteogenic *in vivo* differentiation of human MSC. For clinical application, MSC can well be transplanted in the context of this scaffold since its complete degradation or resorption allows that it can fully be replaced by newly formed bone (Jensen *et al.*, 2006; Okuda *et al.*, 2007). Unfortunately, it was not possible to document and correlate the degree of resorption of β-TCP to proliferation rate, because the radio-opaque shadows of newly built bone obtained by quantitative micro-computed tomography could not be discriminated from those of the ceramic.

Remarkably, enhanced conditions adapted from embryonal stem cell expansion were able to rescue the bone forming ability of inferior MSC in agreement with an enhanced proliferation rate, extending the permissive window to later time points in culture. Overall it is tempting to speculate that, in general, a high anabolism may be a rate limiting parameter crucial for therapeutic applications in which the trophic activity of MSC is important like in myocardial infarction. On top of this, open chromatin may be further relevant if differentiation and thus mesengenic activity is required to allow cells to contribute physically to repair tissue due to their plasticity. In contrast to this, MSC with inhibited proliferation were unable to form bone *in vivo*, showing again the correlation between growth and osteogenic *in vivo* potency. In Fig. 3, at first sight, mitomycin C-treated cells seemed to be half as vital as untreated MSC that may be caused by a toxicity of the reagent. However, these values were not normalised to the DNA content of the wells and generation time at seeding of untreated MSC suggests that cells expanded about two-fold during the assay, while mitomycin C-treated MSC were unable to proliferate. Taking this into consideration,

there is almost no difference in MSC vitality between both groups giving no hints on a toxicity of the chosen standard mitomycin C concentration on MSC.

One important question is why the dominant role of growth for therapeutic potency was so far unrecognised. First, there are only a few studies which systematically addressed the donor variability of primary human MSC in the context of a desired *in vivo* outcome. Among studies addressing donor-dependent features of bone formation (Mendes *et al.*, 2002; Mendes *et al.*, 2004; Siddappa *et al.*, 2007; De Bari *et al.*, 2008) only two studies comprised more than 5 donors and in both a osteogenic pre-induction protocol was applied before transplantation (Mendes *et al.*, 2002; Mendes *et al.*, 2004). Second, opposite to clinical application, where sorting out of inferior cell populations is not possible since the donors require a treatment, researchers frequently work only with the best cell populations leaving those of inferior growth behind. Third, investigators usually do not know the number of multipotent MSC in their starting cultures which can differ by more than 100-fold per mononuclear cell fraction according to colony-forming assays (Majors *et al.*, 1997; Muschler *et al.*, 2001). Thus, some MSC populations may have already undergone 7-10 more population doublings before first confluency compared to others with seeding density being an additional parameter to influence the replicative potential of MSC (Phinney, 2002). Thus, the usual "standardisation" of cultures by passage number falls short in reflecting comparable conditions between donors and may hide this correlation unless a high number of donor populations are investigated, as done in this study.

Although a sharp threshold of around 43 h per population doubling was here suggested to separate bone-forming from non-bone-forming MSC, indeed a time span of several hours existed (between 43 h and about 60 h per population doubling), within which the generation time alone could not fully predict the *in vivo* outcome in the heterotopic model. In single cases, non-cellular parameters related to the mouse or the transplantation procedure may have prevented bone formation as evident from gene expression profiling of MSC from donor 10, which perfectly matched other bone forming samples in cluster analysis of gene expression (Fig. 4), but was unable to form bone *in vivo*. Obviously however, at a still permissive proliferation rate between 43 and 60 h, other factors become relevant which further influence the degree of bone formation *in vivo*. Interestingly, increased overrepresentation of extracellular matrix genes was recently reported to characterise the molecular phenotype of a human MSC clone with bone-forming capacity at lower population level compared to high population level when heterotopic bone formation was lost (Larsen *et al.*, 2010). Since this MSC line grows indefinitely due to stable expression of the human telomerase reverse-transcriptase (hTERT) gene, speed of proliferation may not be rate-limiting allowing extracting further predictors beyond proliferation rate like expression of decorin or natriuretic peptide-receptor-C which were, however, not extracted in our transcriptome analysis.

Genes known as positive regulators of osteogenesis like ALP, Runx2, osteopontin, osteocalcin or bone sialoprotein

were not significantly up-regulated in our gene expression profiling of undifferentiated MSC populations. Before transplantation, there was also no significant difference regarding the expression of osteogenic genes between bone-forming MSC populations and MSC without the ability to form bone. This demonstrates that the contamination of MSC populations with osteoblasts or partly differentiated osteogenic progenitor cells, although present to some extent, was no prominent factor influencing bone formation. This suggests that the high proliferation rate of a large fraction of MSC in a population out-competed the possible advantage by a fraction of cells that may already have taken the first steps to become an osteoblast. The highly ordered deposition of bone towards the β-TCP scaffold pores suggests that the capacity to deposit a mineralised matrix is spatially controlled and the fittest MSC to achieve this may be fast proliferating rather than pre-differentiated cells.

Importantly, *in vitro* mineral deposition did not correlate with the *in vivo* bone formation in our study and this disqualified the standard osteogenic *in vitro* assay as a correlate of heterotopic bone formation ability of human MSC. This is in line with another study showing that *ex vivo* matrix mineralisation assays lack specificity, may be confounded by precipitation of calcium phosphate and show surprisingly poor concordance with bone formation *in vivo* (Larsen *et al.*, 2010). Overall, this questions the usefulness of *in vitro* mineralisation to define "multilineage capacity" of mesenchymal cell populations. In contrast to mineralisation, ALP activity during *in vitro* osteogenesis seemed to be a more specific parameter to predict the osteogenic *in vivo* potency of human MSC. Peak ALP values were chosen for statistical correlation since the time course of ALP up-regulation was distinct between donors, and day 21 provided not always the highest values. Our results showed that optimum *in vitro* ALP activity was a growth-related parameter and highlighted again the correlation to and importance of proliferation.

Altered expansion conditions will require determination of a new threshold level for generation time as predictor, and the heterotopic bone formation model applied here cannot be used to conclude about the bone formation ability of MSC in a bony defect. If bone is formed at an ectopic site in the absence of a supporting bone environment, it is however likely that the same cells will also be able to form bone orthotopically in a bony lesion. Nevertheless, observations from an adequate orthotopic model are required to decide about the importance of high proliferation rate and open chromatin for neo-bone formation in a setting closer to clinical application.

Since age-related changes were reported for human MSC (Stolzing *et al.*, 2008), people with inferior stem cells in bone marrow aspirates might exist. Most importantly our data promise that all aspects ensuring fast but limited expansion of MSC, like use of sufficient MSC at start of culture, enhanced growth conditions, and careful calculation of the number of cells to be transplanted, may pave the way for promising therapeutic application of MSC from elderly donors given a successful potency testing before transplantation.

Conclusion

In conclusion, therapeutic efficiency of MSC may strongly depend on their trophic and mesengenic "fitness" which in our study correlated with a short generation time and, thus, high anabolism. We demonstrated that proliferation of MSC is a rate-limiting determinant of heterotopic bone formation, established a causal relationship between growth and engraftment and introduced a potency test allowing prediction of *in vivo* bone forming ability with high sensitivity and specificity.

Rather than identifying unsuitable donors, we suggest that MSC have to be transplanted in a time window in which sufficient cells show high anabolism as major prerequisite for trophic and mesengenic activity.

Acknowledgements

References

Agata H, Asahina I, Watanabe N, Ishii Y, Kubo N, Ohshima S, Yamazaki M, Tojo A, Kagami H (2010) Characteristic change and loss of *in vivo* osteogenic abilities of human bone marrow stromal cells during passage. Tissue Eng Part A **16**: 663-673.

Bruder SP, Kraus KH, Goldberg VM, Kadiyala S (1998a) The effect of implants loaded with autologous mesenchymal stem cells on the healing of canine segmental bone defects. J Bone Joint Surg Am **80**: 985-996.

Bruder SP, Kurth AA, Shea M, Hayes WC, Jaiswal N, Kadiyala S (1998b) Bone regeneration by implantation of purified, culture-expanded human mesenchymal stem cells. J Orthop Res **16**: 155-162.

Caplan AI (2009) Why are MSCs therapeutic? New data: new insight. J Pathol **217**: 318-324.

De Bari C, Dell'Accio F, Karystinou A, Guillot PV, Fisk NM, Jones EA, McGonagle D, Khan IM, Archer CW, Mitsiadis TA, Donaldson AN, Luyten FP, Pitzalis C (2008) A biomarker-based mathematical model to predict bone-forming potency of human synovial and periosteal mesenchymal stem cells. Arthritis Rheum **58**: 240-250.

Dennis G, Jr., Sherman BT, Hosack DA, Yang J, Gao W, Lane HC, Lempicki RA (2003) DAVID: Database for Annotation, Visualization, and Integrated Discovery. Genome Biol **4**: 3.

Dickhut A, Pelttari K, Janicki P, Wagner W, Eckstein V, Egermann M, Richter W (2009) Calcification or dedifferentiation: requirement to lock mesenchymal stem cells in a desired differentiation stage. J Cell Physiol **219**: 219-226.

Digirolamo CM, Stokes D, Colter D, Phinney DG, Class R, Prockop DJ (1999) Propagation and senescence of human marrow stromal cells in culture: a simple colony-forming assay identifies samples with the greatest potential to propagate and differentiate. Br J Haematol **107**: 275-281.

Eisen MB, Spellman PT, Brown PO, Botstein D (1998) Cluster analysis and display of genome-wide expression patterns. Proc Natl Acad Sci U S A **95**: 14863-14868.

Hernigou P, Mathieu G, Poignard A, Manicom O, Beaujean F, Rouard H (2006) Percutaneous autologous bone-marrow grafting for nonunions. Surgical technique. J Bone Joint Surg Am **88 Suppl 1**: 322-327.

Huang DW, Sherman BT, Lempicki RA (2009) Systematic and integrative analysis of large gene lists using DAVID bioinformatics resources. Nat Protoc **4**: 44-57.

Jaiswal N, Haynesworth SE, Caplan AI, Bruder SP (1997) Osteogenic differentiation of purified, culture-expanded human mesenchymal stem cells *in vitro*. J Cell Biochem **64**: 295-312.

Janicki P, Kasten P, Kleinschmidt K, Luginbuehl R, Richter W (2010) Chondrogenic pre-induction of human mesenchymal stem cells on beta-TCP: enhanced bone quality by endochondral heterotopic bone formation. Acta Biomater **6**: 3292-3301.

Jensen SS, Broggini N, Hjorting-Hansen E, Schenk R, Buser D (2006) Bone healing and graft resorption of autograft, anorganic bovine bone and beta-tricalcium phosphate. A histologic and histomorphometric study in the mandibles of minipigs. Clin Oral Implants Res **17**: 237-243.

Krebsbach PH, Kuznetsov SA, Satomura K, Emmons RV, Rowe DW, Robey PG (1997) Bone formation in vivo: comparison of osteogenesis by transplanted mouse and human marrow stromal fibroblasts. Transplantation **63**: 1059-1069.

Kuznetsov SA, Mankani MH, Robey PG (2000) Effect of serum on human bone marrow stromal cells: *ex vivo* expansion and *in vivo* bone formation. Transplantation **70**: 1780-1787.

Larsen KH, Frederiksen CM, Burns JS, Abdallah BM, Kassem M (2010) Identifying a molecular phenotype for bone marrow stromal cells with in vivo bone-forming capacity. J Bone Miner Res **25**: 796-808.

Lazarus HM, Haynesworth SE, Gerson SL, Caplan AI (1997) Human bone marrow-derived mesenchymal (stromal) progenitor cells (MPCs) cannot be recovered from peripheral blood progenitor cell collections. J Hematother **6**: 447-455.

Majors AK, Boehm CA, Nitto H, Midura RJ, Muschler GF (1997) Characterization of human bone marrow stromal cells with respect to osteoblastic differentiation. J Orthop Res **15**: 546-557.

Mannello F, Tonti GA (2007) Concise review: no breakthroughs for human mesenchymal and embryonic stem cell culture: conditioned medium, feeder layer, or feeder-free; medium with fetal calf serum, human serum, or enriched plasma; serum-free, serum replacement nonconditioned medium, or ad hoc formula? All that glitters is not gold! Stem Cells **25**: 1603-1609.

Martin I, Muraglia A, Campanile G, Cancedda R, Quarto R (1997) Fibroblast growth factor-2 supports *ex*

vivo expansion and maintenance of osteogenic precursors from human bone marrow. Endocrinology **138**: 4456-4462.

Matsushima A, Kotobuki N, Tadokoro M, Kawate K, Yajima H, Takakura Y, Ohgushi H (2009) *In vivo* osteogenic capability of human mesenchymal cells cultured on hydroxyapatite and on beta-tricalcium phosphate. Artif Organs **33**: 474-481.

McLain RF, Fleming JE, Boehm CA, Muschler GF (2005) Aspiration of osteoprogenitor cells for augmenting spinal fusion: comparison of progenitor cell concentrations from the vertebral body and iliac crest. J Bone Joint Surg Am **87**: 2655-2661.

Mendes SC, Tibbe JM, Veenhof M, Bakker K, Both S, Platenburg PP, Oner FC, de Bruijn JD, van Blitterswijk CA (2002) Bone tissue-engineered implants using human bone marrow stromal cells: effect of culture conditions and donor age. Tissue Eng **8**: 911-920.

Mendes SC, Tibbe JM, Veenhof M, Both S, Oner FC, van Blitterswijk CA, de Bruijn JD (2004) Relation between *in vitro* and *in vivo* osteogenic potential of cultured human bone marrow stromal cells. J Mater Sci Mater Med **15**: 1123-1128.

Metz CE, Goodenough DJ, Rossmann K (1973) Evaluation of receiver operating characteristic curve data in terms of information theory, with applications in radiography. Radiology **109**: 297-303.

Muraglia A, Martin I, Cancedda R, Quarto R (1998) A nude mouse model for human bone formation in unloaded conditions. Bone **22**: 131S-134S.

Muschler GF, Boehm C, Easley K (1997) Aspiration to obtain osteoblast progenitor cells from human bone marrow: the influence of aspiration volume. J Bone Joint Surg Am **79**: 1699-1709.

Muschler GF, Nitto H, Boehm CA, Easley KA (2001) Age- and gender-related changes in the cellularity of human bone marrow and the prevalence of osteoblastic progenitors. J Orthop Res **19**: 117-125.

Okuda T, Ioku K, Yonezawa I, Minagi H, Kawachi G, Gonda Y, Murayama H, Shibata Y, Minami S, Kamihira S, Kurosawa H, Ikeda T (2007) The effect of the microstructure of beta-tricalcium phosphate on the metabolism of subsequently formed bone tissue. Biomaterials **28**: 2612-2621.

Phinney DG (2002) Building a consensus regarding the nature and origin of mesenchymal stem cells. J Cell Biochem Suppl **38**: 7-12.

Phinney DG (2007) Biochemical heterogeneity of mesenchymal stem cell populations: clues to their therapeutic efficacy. Cell Cycle **6**: 2884-2889.

Phinney DG, Kopen G, Righter W, Webster S, Tremain N, Prockop DJ (1999) Donor variation in the growth properties and osteogenic potential of human marrow stromal cells. J Cell Biochem **75**: 424-436.

Pietila M, Lehtonen S, Narhi M, Hassinen IE, Leskela HV, Aranko K, Nordstrom K, Vepsalainen A, Lehenkari P (2010) Mitochondrial function determines the viability and osteogenic potency of human mesenchymal stem cells. Tissue Eng Part C Methods **16**: 435-445.

Platt MO, Wilder CL, Wells A, Griffith LG, Lauffenburger DA (2009) Multipathway kinase signatures of multipotent stromal cells are predictive for osteogenic

differentiation: tissue-specific stem cells. Stem Cells **27**: 2804-2814.

Reyes M, Lund T, Lenvik T, Aguiar D, Koodie L, Verfaillie CM (2001) Purification and *ex vivo* expansion of postnatal human marrow mesodermal progenitor cells. Blood **98**: 2615-2625.

Rickard DJ, Kassem M, Hefferan TE, Sarkar G, Spelsberg TC, Riggs BL (1996) Isolation and characterization of osteoblast precursor cells from human bone marrow. J Bone Miner Res **11**: 312-324.

Russell KC, Phinney DG, Lacey MR, Barrilleaux BL, Meyertholen KE, O'Connor KC (2010) *In vitro* high-capacity assay to quantify the clonal heterogeneity in trilineage potential of mesenchymal stem cells reveals a complex hierarchy of lineage commitment. Stem Cells **28**: 788-798.

Shahdadfar A, Fronsdal K, Haug T, Reinholt FP, Brinchmann JE (2005) *In vitro* expansion of human mesenchymal stem cells: choice of serum is a determinant of cell proliferation, differentiation, gene expression, and transcriptome stability. Stem Cells **23**: 1357-1366.

Siddappa R, Licht R, van Blitterswijk C, de Boer J (2007) Donor variation and loss of multipotency during in vitro expansion of human mesenchymal stem cells for bone tissue engineering. J Orthop Res **25**: 1029-1041.

Siddappa R, Martens A, Doorn J, Leusink A, Olivo C, Licht R, van Rijn L, Gaspar C, Fodde R, Janssen F, van Blitterswijk C, de Boer J (2008) cAMP/PKA pathway activation in human mesenchymal stem cells *in vitro* results in robust bone formation *in vivo*. Proc Natl Acad Sci USA **105**: 7281-7286.

Sotiropoulou PA, Perez SA, Salagianni M, Baxevanis CN, Papamichail M (2006) Characterization of the optimal culture conditions for clinical scale production of human mesenchymal stem cells. Stem Cells **24**: 462-471.

Steck E, Burkhardt M, Ehrlich H, Richter W (2010) Discrimination between cells of murine and human origin in xenotransplants by species specific genomic *in situ* hybridization. Xenotransplantation **17**: 153-159.

Stenderup K, Justesen J, Clausen C, Kassem M (2003) Aging is associated with decreased maximal life span and accelerated senescence of bone marrow stromal cells. Bone **33**: 919-926.

Stolzing A, Jones E, McGonagle D, Scutt A (2008) Age-related changes in human bone marrow-derived mesenchymal stem cells: consequences for cell therapies. Mech Ageing Dev **129**: 163-173.

Tarte K, Gaillard J, Lataillade JJ, Fouillard L, Becker M, Mossafa H, Tchirkov A, Rouard H, Henry C, Splingard M, Dulong J, Monnier D, Gourmelon P, Gorin NC, Sensebe L (2010) Clinical-grade production of human mesenchymal stromal cells: occurrence of aneuploidy without transformation. Blood **115**: 1549-1553.

Wagner W, Ho AD (2007) Mesenchymal stem cell preparations – comparing apples and oranges. Stem Cell Rev **3**: 239-248.

Winter A, Breit S, Parsch D, Benz K, Steck E, Hauner H, Weber RM, Ewerbeck V, Richter W (2003) Cartilage-like gene expression in differentiated human stem cell spheroids: a comparison of bone marrow-derived and adipose tissue-derived stromal cells. Arthritis Rheum **48**: 418-429.

Zweig MH, Campbell G (1993) Receiver-operating characteristic (ROC) plots: a fundamental evaluation tool in clinical medicine. Clin Chem **39**: 561-577.

Discussion with Reviewers

Reviewer I: Density gradient isolated bone marrow cells were used in the present study. The authors call these cells "mesenchymal stem cells" but further characterisation is missing (cell surface marker profile, differentiation capacity, minimal criteria, see Dominici *et al.* (2006). It is therefore suggested that these cells are not called "mesenchymal stem cells" but "bone marrow stromal cells". Please comment.

Authors: We call the cells in our study "mesenchymal stem cells" because we routinely screen them for the expression pattern of defined clusters of differentiation as recommended by the International Society for Cellular Therapy (Dominici *et al.*, 2006). We have previously published cell surface marker profiles for MSC from bone marrow, adipose tissue and synovial membrane (Dickhut *et al.*, 2009, text reference). Additionally, we always convince ourselves of the multipotency of the isolated MSC by differentiating the cell populations towards the osteogenic, adipogenic and chonrogenic lineage (Winter *et al.*, 2003, text reference).

Reviewer I: Can you speculate which cells might be more effective for therapeutical use: stem cells or bone marrow stromal cells?

Authors: While bone marrow stromal cells were recognised as the niche cells supporting haematopoietic stem cells in bone, mesenchymal stem cells are naturally found as perivascular cells in many tissues which are released at sites of injury to secrete large quantities of bioactive factors. Since both cell types seem to have the capacity to build up new mesenchymal tissue, the term "mesenchymal stem cell" and "bone marrow stromal cell" is often used as a synonym for a cell population with tissue regeneration potential derived from bone marrow. Due to the lack of a specific marker profile to distinguish bone marrow stromal cells from mesenchymal stem cells it is difficult to tell which cell entity has higher stem cell character. Their effectivity for therapeutic use may depend on many factors, not only on their origin in the body.

Reviewer II: It is known that ALK activity is dependent on the levels of Mg. Did the authors measure the levels of magnesium in the mice as this may have little to do with the stem cells. Mg depletion can reduce ALK phosphatase and osteoblast activity?

Authors: No, we did not measure the level of magnesium in our animals. Since they were fed with magnesium-containing food (0.22 %), we expected physiological levels in all animals, but cannot exclude a magnesium effect on bone formation. Importantly, ALP activity was assessed only *in vitro* in this study and not in the transplanted

β-TCP/MSC-constructs, thus here a magnesium effect can be excluded.

Reviewer II: Why did mitomycin-treated cells deposit a mineralised matrix *in vitro*?
Authors: Mitomycin C-treated MSC were shown to be unable to proliferate on the one hand but were still vital as shown by the WST assay (see Fig. 3). Consequently, when cells are vital, they are able to answer to extrinsic stimuli like induction media. In our case, MSC answered to osteogenic *in vitro* stimuli showing that proliferation was not necessary for the deposition of calcified matrix. This was in sharp contrast to the *in vivo* situation where the ability to proliferate was essential for successful bone formation and showed again, that the *in vitro* mineralisation assay is not informative about the bone forming potency of human MSC.

Reviewer II: Wouldn't it be better to use clones?
Authors: We used non-clonal MSC populations to be close to the clinical situation. Cloning is unattractive since MSC clones are not stable. So after expansion of clones, one ends up with a heterogeneous cell population derived from one cell.

Reviewer II: The conclusions are based on the scaffold and have very little to do with the clinic. Please comment.
Authors: Our conclusion is based on a scaffold with high osteo-permissive features which were demonstrated and compared in a previous study (Janicki *et al*., 2010, text reference). Human MSC do not form ectopic bone without any scaffold. Thus, we made the decision to choose β-TCP as a matrix frequently used in orthopaedic surgery. MSC could well be transplanted in context with such granules in patients.

Additional Reference

Dominici M, Le Blanc K, Mueller I, Slaper-Cortenbach I, Marini F, Krause D, Deans R, Keating A, Prockop Dj, Horwitz E (2006) Minimal criteria for defining multipotent mesenchymal stromal cells. The International Society for Cellular Therapy position statement. Cytotherapy **8**: 315-317.